PHOTONICS Research

"Periodic" soliton explosions in a dual-wavelength mode-locked Yb-doped fiber laser

Meng Liu,[1] Ti-Jian Li,[1] Ai-Ping Luo,[1] (iD) Wen-Cheng Xu,[1,2] and Zhi-Chao Luo[1,3] (iD)

[1]Guangzhou Key Laboratory for Special Fiber Photonic Devices and Applications & Guangdong Provincial Key Laboratory of Nanophotonic Functional Materials and Devices, South China Normal University, Guangzhou 510006, China
[2]e-mail: xuwch@scnu.edu.cn
[3]e-mail: zcluo@scnu.edu.cn

We report the "periodic" soliton explosions induced by intracavity soliton collisions in a dual-wavelength mode-locked Yb-doped fiber laser. Owing to the different group velocities of the two wavelengths, the mode-locked solitons centered at different wavelengths would periodically collide with each other. By using the dispersive Fourier transformation technique, it was found that each collision would induce soliton explosions, but none of them would be identical. Therefore, this phenomenon was termed as "periodic" soliton explosions. In addition, the dissipative rogue waves were detected in the dual-wavelength mode-locked state. The experimental results would be fruitful to the communities interested in soliton dynamics and dual-comb lasers.   © 2020 Chinese Laser Press

1. INTRODUCTION

As efficient pulse sources, ultrafast fiber lasers have been applied to many fields such as laser processing and optical communication [1,2]. In addition, due to the dissipative feature of ultrafast fiber lasers and they have been regarded as great platforms to investigate nonlinear phenomena and soliton dynamics. So far, by selecting cavity parameters, various types of soliton dynamics have been observed in ultrafast fiber lasers, such as dissipative soliton resonance [3–6], harmonic mode-locked solitons [7,8], and vector solitons [9–13]. Most of these soliton dynamics in ultrafast fiber lasers are stationary or quasi-stationary states. Besides that, the fiber laser could also operate in the transient states with some certain cavity parameters. Since the dispersive Fourier transformation (DFT) technique was introduced into soliton dynamic research as a real-time spectroscopy technique, soliton transient dynamics have gained more and more attention because of their fruitful nonlinear phenomena and potential practical applications. Indeed, by using the DFT technique, versatile soliton transient dynamics have been observed in fiber lasers, such as soliton buildup [14–18], evolving soliton molecules [19,20], rogue waves [21,22], soliton explosions [23–25], and pulsating solitons [26,27].

Among them, soliton explosions could be regarded as one of the most fantastic phenomena, in which solitons intermittently suffer explosive instabilities and then recover to their original status after each explosion [28–31]. Until now, many efforts have been devoted to investigation of the soliton explosions.

The earlier numerical results have demonstrated that the higher-order effects play important roles in the generation and characteristics of soliton explosions [30,32]. In 2015 the real-time dynamics of soliton explosions were first observed in a fiber laser by using the DFT technique [23], and the experimental investigations on soliton explosions were greatly stimulated. Soliton explosions have been demonstrated to exist in different operation wavebands with different mode-locking techniques [23–25,33–37]. In general, the phenomenon of soliton explosion in fiber lasers is related to the cavity nonlinear effect, which could be regarded as a transition state between a stable state and a noise-like state. The typical characteristic of soliton explosion is the abrupt collapse of the soliton spectrum and the recovery of the stable state soon after that. In some cases, the temporal shift of pulse, Raman components, and dissipative rogue waves (DRWs) would occur accompanying the soliton explosion [23,24]. The duration of soliton explosion could vary from several to thousands of round-trips with certain cavity parameters. Up to now, most of the reports have been focused on the explosion of single soliton. As for the explosion of multi-solitons, Yu et al. found that explosion of one soliton could be ignited by another one through the soliton interactions mediated by the transient gain response of an erbium-doped fiber [36].

So far, all the soliton explosions mentioned above appeared randomly and were observed in single-wavelength mode-locked fiber lasers. As we know, dual-wavelength mode-locked solitons would periodically collide with each other due to the different

group velocities of different wavelengths. It has been demonstrated that the soliton collisions that happened in ultrafast fiber lasers exhibited various fantastic behaviors such as soliton molecule formation, soliton fusion or annihilation, and energy exchange [38]. In addition, it has been theoretically confirmed that soliton collisions would induce soliton explosion in the framework of two coupled cubic-quintic complex Ginzburg–Landau equations for counter-propagating waves [39]. Then it is interesting to see whether a soliton collision in dual-wavelength fiber lasers could induce soliton explosion and whether the periodic collisions of dual-wavelength solitons would lead to periodic soliton explosions. On the other hand, dual-wavelength mode-locked fiber lasers have potential applications in many fields such as optical instrumentation, wavelength-division multiplexing (WDM) networks, and optical sensing. Furthermore, they could be regarded as a promising optical source for dual-comb spectroscopy [40,41]. However, the inevitable soliton collisions in the laser cavity may have great influence on the performance of the dual-wavelength mode-locked fiber laser. Therefore, it is meaningful to investigate the dynamics of dual-wavelength solitons in ultrafast fiber lasers.

In this work, we conducted a dual-wavelength Yb-doped fiber (YDF) laser mode locked by a semiconductor saturable absorber (SA). The two wavelengths are ~1061.38 nm and ~1063.16 nm. By employing the DFT technique, the "periodic" soliton explosions could be observed just after each collision. Both solitons would experience "periodic" explosions, but none of the explosions would be identical. During the dual-wavelength mode-locked state, extremely high-amplitude waves, which were also confirmed as DRWs, appeared with small probability after the DFT process. These results could not only shed new light on the dynamics of soliton explosions and soliton collisions but also be of great significance in the fields of both physical research and industrial applications.

2. EXPERIMENTAL SETUP

The schematic of the YDF laser is shown in Fig. 1. As the gain medium, a piece of ~1 m YDF (Nufern SM-YSF-HI) is pumped by a 975 nm laser diode through a 980/1060 nm wavelength-division multiplexer. The other fibers in the laser cavity are ~71 m HI-1060 fiber. Thus, the whole cavity length is about ~72 m.

In order to obtain stable mode-locking operation in the all-normal-dispersion regime, a fiber-pigtailed bandpass filter
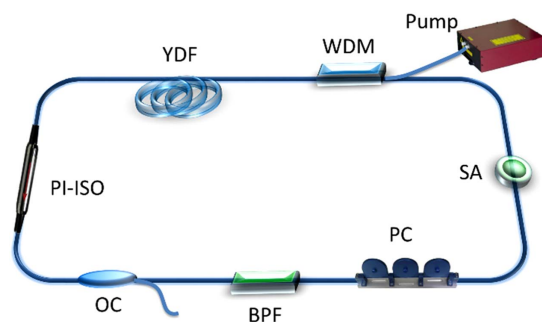
(BPF) centered at 1060 nm with a bandwidth of 5 nm is inserted into the cavity [42]. The unidirectional operation is ensured by a polarization-independent isolator (PI-ISO). A polarization controller (PC) is employed to adjust the polarization state of the circulating light. The mode-locking operation is realized by a commercial semiconductor SA (BATOP 1064-26-37ps). The laser output is taken by a 20% fiber coupler, which is simultaneously measured by an optical spectrum analyzer (OSA, Anritsu MS9710C) and a high-speed real-time oscilloscope (Tektronix DSA-70804, 8 GHz) with a photodetector (Newport 818-BB-35F, 12.5 GHz). In addition, a ~15 km standard single-mode fiber (SMF) is placed between the oscilloscope and the output coupler (OC) to realize the DFT technique. Then the real-time spectral characteristics of the solitons with a spectral resolution of ~0.29 nm [43–45] could be observed.

3. EXPERIMENTAL RESULTS

By virtue of the saturable absorption of the semiconductor SA, the self-mode-locking operation could be easily achieved by increasing the pump power to 125 mW. Figure 2 summarizes the performance of stable single-wavelength mode-locked state. Due to the all-normal cavity dispersion, a typical rectangular spectrum of the dissipative soliton could be obtained in our fiber laser as shown in Fig. 2(a). The center wavelength and 10 dB bandwidth of the mode-locked spectrum are ~1061.38 nm and ~2.57 nm, respectively. Figure 2(b) shows the corresponding pulse train, whose pulse interval is ~351.43 ns. The pulse duration is measured to be ~86 ps by an autocorrelator as presented in the inset of Fig. 2(b). Moreover, the radio frequency (RF) spectrum of the mode-locked soliton was measured as shown in Fig. 2(c). The peak located at the frequency of 2.8455 MHz represents the fundamental repetition rate, which has a signal-to-noise ratio of >70 dB. In order to verify the stability of the mode-locking operation, the shot-to-shot spectra with 1000 round-trips were measured by virtue of the DFT technique as presented in Fig. 2(d). Here we can clearly see that the intensities and profiles of the shot-to-shot spectra remain almost unchanged. The results demonstrated that the laser was operating in the stable single-wavelength mode-locked state.

As we know, the spectral filter effect could be generated by the combination of the intracavity birefringence and the polarization-dependent loss [46]. By adjusting the PC and pump power, the parameters of the spectral filter, such as the transmission peaks at different wavelengths and free spectral range, could be changed. Therefore, in our experiments, dual-wavelength operation could be achieved by adjusting the PC and pump power. The red solid line in Fig. 3(a) shows the spectrum of the dual-wavelength mode-locked state at the pump power of 131.5 mW. The two lasing wavelengths are estimated to be at ~1061.38 nm and ~1063.16 nm, respectively, since there is a small overlap between the two spectra. The corresponding pulse trains are presented in Fig. 3(b), where we can see that there are two sets of pulse trains with different intensities. By carefully analyzing the pulse trains in Fig. 3(b), the pulse train with higher intensity is at ~1061.38 nm, while the other one is at ~1063.16 nm. Figure 3(c) provides the
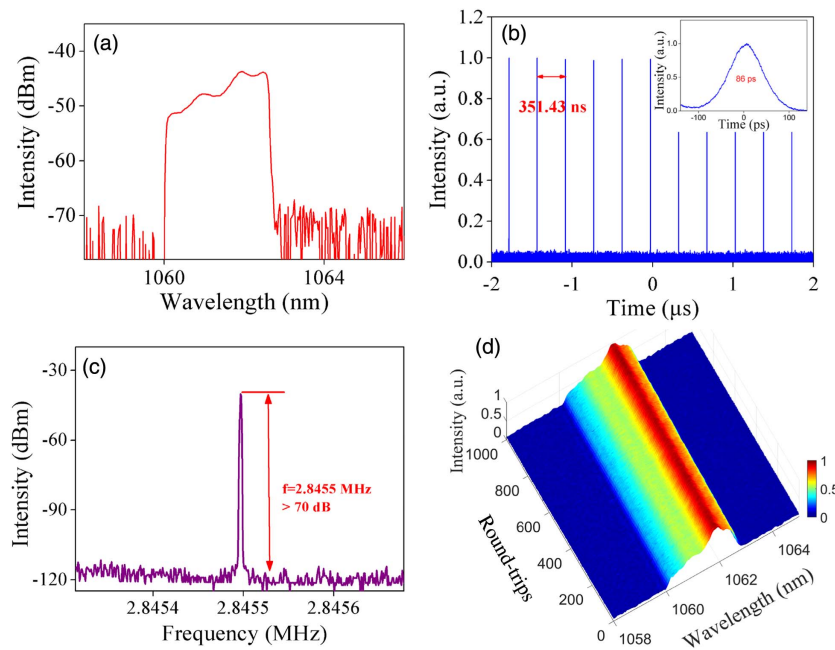

Fig. 1. Schematic of the Yb-doped fiber laser in this experiment.

Fig. 2. Single-wavelength mode-locking operation. (a) Spectrum; (b) pulse train, inset: autocorrelation trace; (c) RF spectrum; (d) shot-to-shot spectra with 1000 round-trips.

RF spectrum in this state, where there are two peaks with an interval of ~40.81 Hz. The autocorrelation trace measured in this state shows that the pulse duration is ~108 ps. Since different wavelengths have different group velocities, the dual-wavelength mode-locked solitons would periodically collide with each other. The collision period Δt can be calculated by $\Delta t = 1/\Delta f$, where Δf is the difference of the two fundamental repetition rates at two wavelengths. Then the collision period is calculated to be ~24.50 ms. In order to investigate the

soliton collision evolution, we recorded the pulse trains before and after the DFT process during the whole collision process by an oscilloscope as shown in Figs. 3(d) and 3(e). The corresponding pulse evolutions can be found in Visualization 1 and Visualization 2. Moreover, in order to present the evolution more clearly, Fig. 4 shows the pulses of several typical round-trips before and after DFT during the soliton collision process. Here the horizontal axes in Figs. 3(e) and 4(b) are time, rather than wavelength, which is because there are two pulses with
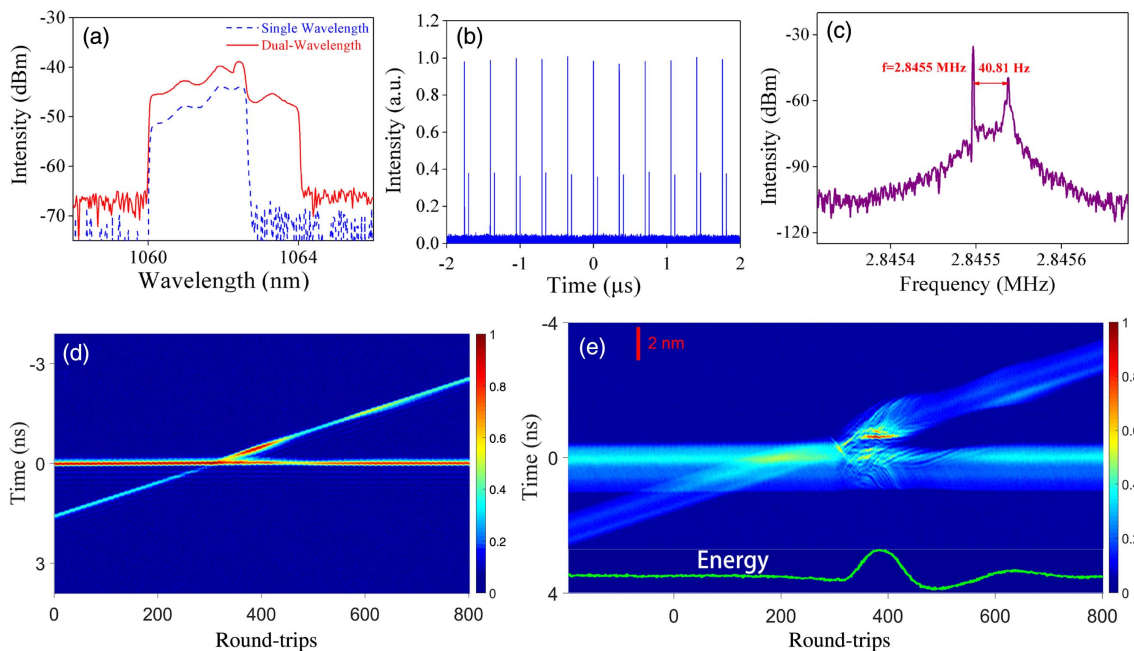

Fig. 3. Dual-wavelength mode-locking operation. (a) Spectrum; (b) pulse train; (c) RF spectrum; (d) pulse evolution before the DFT process (see Visualization 1); (e) stretched pulse evolution after the DFT process (see Visualization 2), inset: pulse energy.
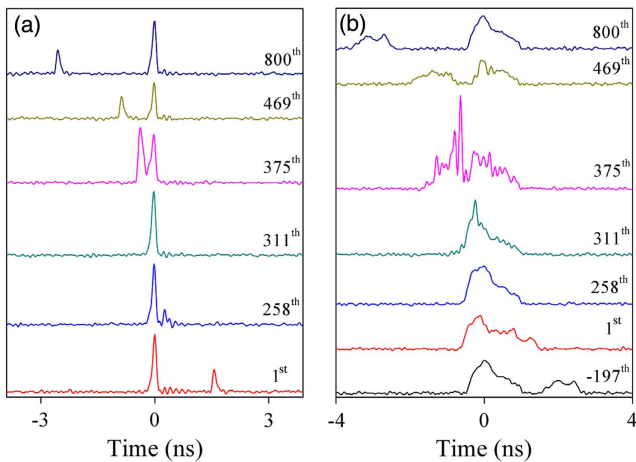
Fig. 4. Pulses (a) before and (b) after the DFT process of several typical round-trips during the soliton collision process.

evolving pulse intervals. However, Figs. 3(e) and 4(b) can still represent the spectral evolution of the two solitons due to the DFT technique. Moreover, it should be noted that in this experiment, ~15 km SMF was used to realize the DFT technique, which led to ~198 round-trips difference between the pulses before and after the DFT process. Namely, when the pulses before and after the DFT process were recorded simultaneously by the oscilloscope, the pulse at the first round-trip corresponded to the DFT-stretched pulse at the 199th round-trip. In Figs. 3(d) and 3(e), the round-trip difference induced by the DFT process has been corrected. However, in order to show the whole collision process, the DFT-stretched pulses from the –197th to the zeroth round-trip are also provided here.

As we know, if soliton interaction occurs, it will be reflected on the pulse intensity and the variation in pulse energy of one round-trip. From the real-time dynamics in Figs. 3(d) and 3(e), it can be found that at first the two solitons move towards each other without interaction from the first to the ~195th round-trip. In Fig. 3(e), from the –100th round-trip on, there is an overlap between the spectra of the two lasing wavelengths; however, it is just the intensity superposition without interaction. The reason is that from the ~ –100th to the ~195th round-trip, the interval between the two solitons was still too large for interaction, which can be identified by the corresponding pulse evolution in Fig. 3(d). In the inset of Fig. 3(e), it can be seen that the energy remains constant during the –197th to the ~195th round-trip, which further confirms that no evident interaction exists in this stage.

Then the two solitons entered the interaction regime. Since the ~195th round-trip, the intensity of the pulse at ~1063.16 nm decreased slightly, as well as the whole energy. The collision between two solitons happens at the ~304th round-trip. In the spectral domain, after the soliton collision, the spectrum collapsed into many spikes, which could be attributed to the perturbation induced by the soliton collision. Then the spectral spikes evolve randomly with changing intensities and numbers. After the ~420th round-trip, the spectra began to restore their structures slowly. The bandwidth of the spectrum at ~1063.16 nm shows obvious variation during the

restoration process. Until the ~770th round-trip, the two solitons totally recover their initial states. In the time domain, just after the collision, the intensity of the soliton at ~1063.16 nm is slightly lower than that of the other soliton as shown in Visualization 1. Then the two solitons experience two energy-exchange processes. In the first one, from the ~339th to the ~365th round-trip, the intensity of the soliton at ~1063.16 nm gradually exceeds that of the other soliton. From the ~365th to the ~770th round-trip, the two solitons exchange their energy again, and finally the soliton with higher intensity is at ~1061.38 nm and the lower one is at ~1063.16 nm, which is consistent with the corresponding intensities of the two solitons at the first round-trip. It is fascinating that the two solitons can be totally restored to their stable initial intensities after the drastic collision, which might contribute to the self-organization effect. In addition, the energy evolution in the inset of Fig. 3(e) shows that the energy increases quickly from the ~304th to the ~390th round-trip, then sharply decreases to the level (~440th round-trip) slightly below the stable state, and at last the energy returns to the stable energy level after a small oscillation. The two solitons, which have exactly the same parameters as the initial state, propagate stably in the laser cavity after all the processes. Considering all the evolution processes, the spectra of the two solitons experienced a stable state, a spectral collapse, and finally a recovery of the stable state, which is in agreement with the characteristics of the soliton explosion phenomenon. Therefore, it could be identified that the soliton explosion induced by the soliton collision was observed in the dual-wavelength mode-locked fiber laser. Moreover, it should be noted that the phase shift induced by the soliton collision process could not be identified in our experimental observations.

Since there is fixed group velocity difference between the two solitons, periodic collisions will happen. Figure 5(a) offers a pulse train after the DFT process with large time range, where it can be seen that the collisions indeed happen within a period of ~24.5 ms. Then it is interesting to see whether each soliton collision can lead to the soliton explosion. We recorded several collision processes, and two of them are shown in Figs. 5(b) and 5(c). It can be seen that soliton explosions will appear after each soliton collision; however, the explosion details are not identical. It is further confirmed that the phenomenon is a soliton explosion. Although the soliton explosions are not the same as each other, an explosion will certainly appear after every periodic soliton collision. Therefore, we can term it "periodic" soliton explosion.

On the other hand, as mentioned above, in some cases the DRWs appear accompanying the soliton explosions [33]. In our experiments, the extremely high-amplitude waves can be observed on the oscilloscope occasionally after the DFT process. Then, for the purpose of verifying whether these waves are DRWs, we recorded 100,000 peak amplitudes of the shot-to-shot DFT-stretched nanosecond pulses at the dual-wavelength mode-locked state and added them to a histogram. Note that the recording process took almost 6 h. Figure 6 displays the statistical distribution histogram recorded for the amplitude fluctuations in a dual-wavelength mode-locked state. The distribution exhibits a long-tailed distribution, meaning that the majority of the
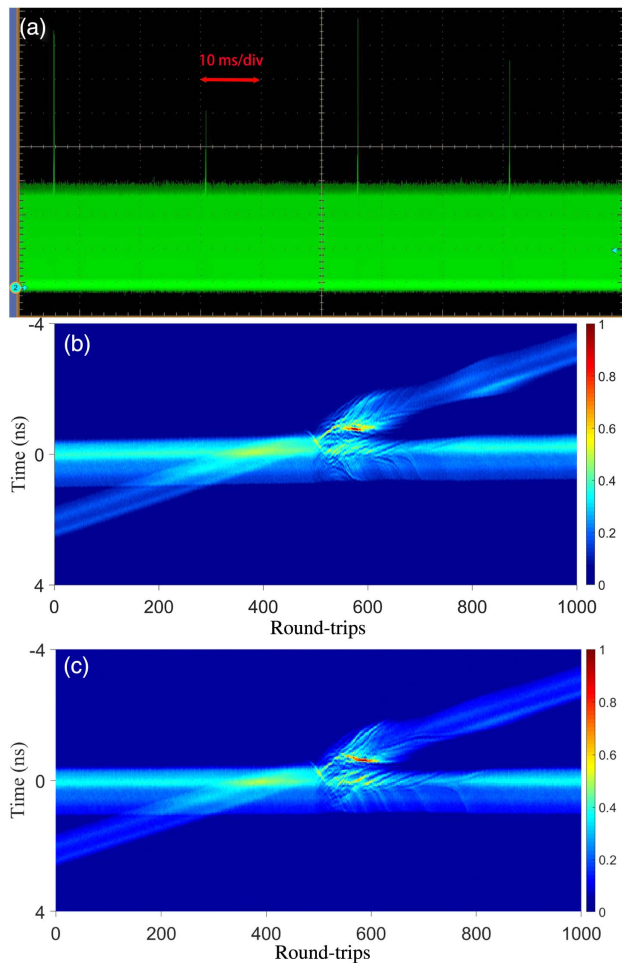
Fig. 5. (a) Pulse train after the DFT process with a large time range; (b), (c) two other soliton collision processes.

amplitude events are concentrated in a lower intensity and the extremely high amplitudes appear rarely. In the histogram, the significant wave height (SWH) is calculated to be ∼0.219 V, and the highest recorded amplitude is about 1.07 V, which reaches ∼4.88 times that of the SWH. It should be noted that each recorded peak amplitude is the highest value of both solitons. Therefore, it could
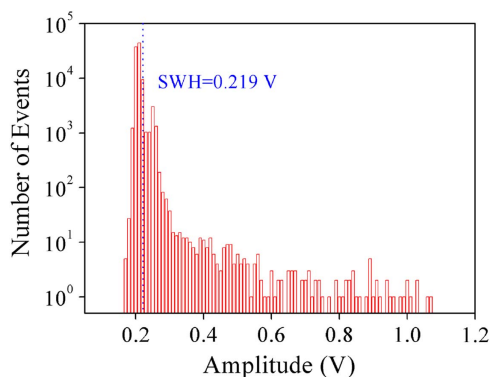

Fig. 6. Intensity histogram on log scale of dual-wavelength state. SWH is ∼0.219 V.

be confirmed that the DRWs have been generated from the dual-wavelength mode-locked fiber laser [21,33,47].

4. DISCUSSION

In our experiment, due to the group velocity difference, the two solitons at different wavelengths periodically collided with each other. The soliton collisions further induced soliton explosions. Although the exploding process never repeated itself exactly, it still could be termed "periodic" soliton explosion due to the periodic occurrence of the soliton collision. In fact, the soliton collision could lead to energy variation, which further influences the cavity nonlinear effect of each soliton. Then the stable solitons experienced instability and exploded. Finally, after the collision, due to the self-stabilization effect, the solitons recovered to their initial states and remained stable until the next collision happened. During the soliton explosion, the spectra collapsed into many spikes, as well as the pulses. The broken small pulses interacted with each other, which rarely generated waves with extremely high amplitude, namely, DRWs.

As we know, dual-wavelength mode-locked fiber lasers have been regarded as optical sources for many applications. However, the inevitable soliton collisions together with soliton explosions actually have negative influence on the performance of dual-wavelength fiber lasers. In addition, the DRWs generated during the soliton explosions are detrimental to laser systems since the waves with extremely high amplitude might burn out the fiber devices, especially in high-power pulsed laser systems. Therefore, more efforts need to be made in dual-wavelength mode-locked fiber lasers. In addition, the dispersion of the fiber laser is essential to the laser's performance. In this work the soliton collision happens in the YDF laser with all-normal dispersion, and further laser cavity design with anomalous dispersion or dispersion management for dual-wavelength mode-locked solitons is required to fully unveil the dynamics of soliton collisions.

5. CONCLUSION

In summary, we demonstrated that "periodic" soliton explosions are induced by the periodic soliton collisions in a dual-wavelength mode-locked YDF laser. None of the soliton explosions repeat themselves exactly in successive collision periods. By analyzing the statistical intensity histogram in dual-wavelength mode-locked state, the DRWs have been proved to be detected in our fiber laser. These results could enhance our understanding of soliton explosions, soliton collisions, and DRWs.

Disclosures. The authors declare no conflicts of interest.

REFERENCES

1. U. Keller, "Recent developments in compact ultrafast lasers," Nature **424**, 831–838 (2003).
2. M. E. Fermann and I. Hartl, "Ultrafast fibre lasers," Nat. Photonics **7**, 868–874 (2013).
3. W. Chang, A. Ankiewicz, J. M. Soto-Crespo, and N. Akhmediev, "Dissipative soliton resonances," Phys. Rev. A **78**, 023830 (2008).
4. X. Wu, D. Y. Tang, H. Zhang, and L. M. Zhao, "Dissipative soliton resonance in an all-normal-dispersion erbium-doped fiber laser," Opt. Express **17**, 5580–5584 (2009).
5. P. Grelu, W. Chang, A. Ankiewicz, J. M. Soto-Crespo, and N. Akhmediev, "Dissipative soliton resonance as a guideline for high-energy pulse laser oscillators," J. Opt. Soc. Am. B **27**, 2336–2341 (2010).
6. Z. C. Luo, W. J. Cao, Z. B. Lin, Z. R. Cai, A. P. Luo, and W. C. Xu, "Pulse dynamics of dissipative soliton resonance with large duration-tuning range in a fiber ring laser," Opt. Lett. **37**, 4777–4779 (2012).
7. C. S. Jun, S. Y. Choi, F. Rotermund, B. Y. Kim, and D. I. Yeom, "Toward higher-order passive harmonic mode-locking of a soliton fiber laser," Opt. Lett. **37**, 1862–1864 (2012).
8. G. Sobon, J. Sotor, and K. M. Abramski, "Passive harmonic mode-locking in Er-doped fiber laser based on graphene saturable absorber with repetition rates scalable to 2.22 GHz," Appl. Phys. Lett. **100**, 161109 (2012).
9. S. T. Cundiff, B. C. Collings, N. N. Akhmediev, J. M. Soto-Crespo, K. Bergman, and W. H. Knox, "Observation of polarization-locked vector solitons in an optical fiber," Phys. Rev. Lett. **82**, 3988–3991 (1999).
10. C. Mou, S. Sergeyev, A. Rozhin, and S. Turistyn, "All-fiber polarization locked vector soliton laser using carbon nanotubes," Opt. Lett. **36**, 3831–3833 (2011).
11. J. H. Wong, K. Wu, H. H. Liu, C. Ouyang, H. Wang, Sh. Aditya, P. Shum, S. N. Fu, E. J. R. Kelleher, A. Chernov, and E. D. Obraztsova, "Vector solitons in a laser passively mode-locked by single-wall carbon nanotubes," Opt. Commun. **284**, 2007–2011 (2011).
12. C. B. Mou, S. V. Sergeyev, A. G. Rozhin, and S. K. Turitsyn, "Bound state vector solitons with locked and precessing states of polarization," Opt. Express **21**, 26868–26875 (2013).
13. Z. C. Wu, D. M. Liu, S. N. Fu, L. Li, M. Tang, and L. M. Zhao, "Scalar-vector soliton fiber laser mode-locked by nonlinear polarization rotation," Opt. Express **24**, 18764–18771 (2016).
14. G. Herink, B. Jalali, C. Ropers, and D. Solli, "Resolving the build-up of femtosecond mode-locking with single-shot spectroscopy at 90 MHz frame rate," Nat. Photonics **10**, 321–326 (2016).
15. X. Wei, B. Li, Y. Yu, C. Zhang, K. K. Tsia, and K. K. Y. Wong, "Unveiling multiscale laser dynamics through time-stretch and time-lens spectroscopies," Opt. Express **25**, 29098–29120 (2017).
16. H. J. Chen, M. Liu, J. Yao, S. Hu, J. B. He, A. P. Luo, W. C. Xu, and Z. C. Luo, "Buildup dynamics of dissipative soliton in an ultrafast fiber laser with net-normal dispersion," Opt. Express **26**, 2972–2982 (2018).
17. P. Ryczkowski, M. Närhi, C. Billet, J. M. Merolla, G. Genty, and J. M. Dudley, "Real-time full-field characterization of transient dissipative soliton dynamics in a mode-locked laser," Nat. Photonics **12**, 221–227 (2018).
18. X. M. Liu, X. K. Yao, and Y. D. Cui, "Real-time observation of the buildup of soliton molecules," Phys. Rev. Lett. **121**, 023905 (2018).
19. G. Herink, F. Kurtz, B. Jalali, D. R. Solli, and C. Ropers, "Real-time spectral interferometry probes the internal dynamics of femtosecond soliton molecules," Science **356**, 50–54 (2017).
20. K. Krupa, K. Nithyanandan, U. Andral, P. Tchofo-Dinda, and P. Grelu, "Real-time observation of internal motion within ultrafast dissipative optical soliton molecules," Phys. Rev. Lett. **118**, 243901 (2017).
21. C. Lecaplain, P. Grelu, J. M. Soto-Crespo, and N. Akhmediev, "Dissipative rogue waves generated by chaotic pulse bunching in a mode-locked laser," Phys. Rev. Lett. **108**, 233901 (2012).
22. Z. W. Liu, S. M. Zhang, and F. W. Wise, "Rogue waves in a normal-dispersion fiber laser," Opt. Lett. **40**, 1366–1369 (2015).
23. A. F. J. Runge, N. G. R. Broderick, and M. Erkintalo, "Observation of soliton explosions in a passively mode-locked fiber laser," Optica **2**, 36–39 (2015).
24. M. Liu, A. P. Luo, Y. R. Yan, S. Hu, Y. C. Liu, H. Cui, Z. C. Luo, and W. C. Xu, "Successive soliton explosions in an ultrafast fiber laser," Opt. Lett. **41**, 1181–1184 (2016).
25. K. Krupa, K. Nithyanandan, and P. Grelu, "Vector dynamics of inco-herent dissipative optical solitons," Optica **4**, 1239–1244 (2017).
26. H. J. Chen, Y. J. Tan, J. G. Long, W. C. Chen, W. Y. Hong, H. Cui, A. P. Luo, Z. C. Luo, and W. C. Xu, "Dynamical diversity of pulsating solitons in a fiber laser," Opt. Express **27**, 28507–28522 (2019).
27. J. S. Peng, S. Boscolo, Z. H. Zhao, and H. P. Zeng, "Breathing dis-sipative solitons in mode-locked fiber lasers," Sci. Adv. **5**, eaax1110 (2019).
28. N. Akhmediev and J. M. Soto-Crespo, "Exploding solitons and Shil'nikov's theorem," Phys. Lett. A **317**, 287–292 (2003).
29. N. Akhmediev and J. M. Soto-Crespo, "Strongly asymmetric soliton explosions," Phys. Rev. E **70**, 036613 (2004).
30. S. C. V. Latas and M. F. S. Ferreira, "Soliton explosion control by higher-order effects," Opt. Lett. **35**, 1771–1773 (2010).
31. O. Descalzi and H. R. Brand, "Transition from modulated to exploding dissipative solitons: hysteresis, dynamics, and analytic aspects," Phys. Rev. E **82**, 026203 (2010).
32. S. C. V. Latas and M. F. S. Ferreira, "Why can soliton explosions be controlled by higher-order effects?" Opt. Lett. **36**, 3085–3087 (2011).
33. M. Liu, A. P. Luo, W. C. Xu, and Z. C. Luo, "Dissipative rogue waves induced by soliton explosions in an ultrafast fiber laser," Opt. Lett. **41**, 3912–3915 (2016).
34. P. Wang, X. Xiao, H. Zhao, and C. Yang, "Observation of duration-tunable soliton explosion in passively mode-locked fiber laser," IEEE Photon. J. **9**, 1507008 (2017).
35. M. Suzuki, O. Boyraz, H. Asghari, P. Trinh, H. Kuroda, and B. Jalali, "Spectral periodicity in soliton explosions on a broadband mode-locked Yb fiber laser using time-stretch spectroscopy," Opt. Lett. **43**, 1862–1865 (2018).
36. Y. Yu, Z. C. Luo, J. Q. Kang, and K. K. Y. Wong, "Mutually ignited soliton explosions in a fiber laser," Opt. Lett. **43**, 4132–4135 (2018).
37. J. Peng and H. Zeng, "Soliton collision induced explosions in a mode-locked fibre laser," Commun. Phys. **2**, 34 (2019).
38. J. K. Jang, M. Erkintalo, K. Luo, G.-L. Oppo, S. Coen, and S. G. Murdoch, "Controlled merging and annihilation of localised dissipative structures in an AC-driven damped nonlinear Schrödinger system," New J. Phys. **18**, 033034 (2016).
39. O. Descalzi and H. R. Brand, "Collisions of non-explosive dissipative solitons can induce explosions," Chaos **28**, 075508 (2018).
40. I. Coddington, N. Newbury, and W. Swann, "Dual-comb spectros-copy," Optica **3**, 414–426 (2016).
41. X. Zhao, G. Hu, B. Zhao, C. Li, Y. Pan, Y. Liu, T. Yasui, and Z. Zheng, "Picometer-resolution dual-comb spectroscopy with a free-running fiber laser," Opt. Express **24**, 21833–21845 (2016).
42. A. Chong, W. H. Renninger, and F. W. Wise, "Properties of normal-dispersion femtosecond fiber lasers," J. Opt. Soc. Am. B **25**, 140–148 (2008).
43. Y. C. Tong, L. Y. Chang, and H. K. Tsang, "Fibre dispersion or pulse spectrum measurement using a sampling oscilloscope," Electron. Lett. **33**, 983–985 (1997).
44. K. Goda and B. Jalali, "Dispersive Fourier transformation for fast con-tinuous single-shot measurements," Nat. Photonics **7**, 102–112 (2013).
45. A. F. J. Runge, C. Aguergaray, N. G. R. Broderick, and M. Erkintalo, "Coherence and shot-to-shot spectral fluctuations in noise-like ultra-fast fiber lasers," Opt. Lett. **38**, 4327–4330 (2013).
46. H. Zhang, D. Y. Tang, X. Wu, and L. M. Zhao, "Multi-wavelength dissipative soliton operation of an erbium-doped fiber laser," Opt. Express **17**, 12692–12697 (2009).
47. Z. R. Cai, M. Liu, S. Hu, J. Yao, A. P. Luo, Z. C. Luo, and W. C. Xu, "Graphene-decorated microfiber photonic device for generation of rogue waves in a fiber laser," IEEE J. Sel. Top. Quantum Electron. **23**, 0900306 (2017).